

Boosting catalytic performance of MOFs for steroid transformations by confinement within mesoporous scaffolds

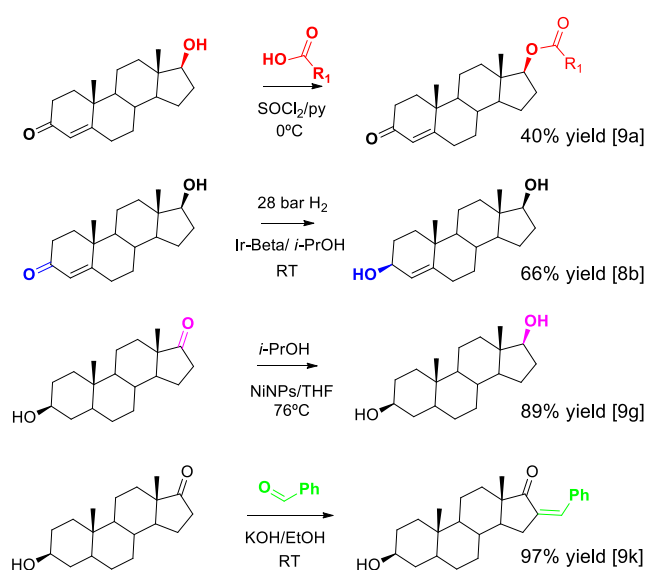
Francisco G. Cirujano*^[a], Ignacio Luz^[b], Mustapha Soukri*^[b], Cedric Van Goethem^[a], Ivo F.J. Vankelecom^[a], Marty Lail^[b] and Dirk E. De Vos*^[a]

Abstract: Selective confinement of MOF nanocrystals within mesoporous materials via novel 'solid state' crystallization provides more accessible active sites compared to the bulk MOF counterpart, enhancing chemical and mechanical stability of MOF nanocrystals. (Zr)UiO-66(NH₂)/SiO₂ hybrid materials were tested as efficient and reusable heterogeneous catalysts for the synthesis of steroid derivatives, outperforming the bulk (Zr)UiO-66(NH₂) MOF. A clear correlation between catalytic activity of the dispersed Zr sites present in the confined MOF and the loading of the mesoporous SiO₂ is demonstrated for steroid transformations.

Porous crystalline metal-organic frameworks (MOFs) composed of inorganic secondary building units (SBUs) interlinked by organic polytopic ligands have been extensively explored during the last decade as promising heterogeneous catalysts.^[1] Defective sites in the crystal are considered the active sites in 'non-post-modified' MOF catalysts. Several synthetic strategies have been recently developed to enhance the generation of such defect sites in MOFs during their crystallization.^[2] Nevertheless, the concentration of defect sites incorporated in those materials is usually inherently limited since the framework stability directly depends on the coordination number of the SBUs. Therefore, new directions must be explored to achieve a fair compromise between activity and stability of MOF catalysts.

In this sense, the selective growth of MOF nanocrystals within mesoporous materials (MPMs) via novel 'solid-state' crystallization allows for an outstanding loading of the mesoporous cavities with very small MOF nanocrystals.^[3] This approach addresses key challenges that MOFs are experiencing as heterogeneous catalysts. On the one hand, the concentration of coordination vacancies at the outer crystal surface is maximized by reducing the MOF crystalline domain down to a few nanometers via confinement within the mesoporous scaffold, without decreasing their inherent activity. On the other hand, the matrix protects and confers additional stability, as well as handling, to the highly active MOF nanocrystals used as catalysts.

In order to demonstrate these advantages, zirconium containing MOF nanocrystals have been confined within mesoporous silica materials. The composite hybrid materials are employed as active, selective and stable heterogeneous catalysts for the conversion of large molecules exhibiting low diffusion coefficients, such as testosterone and epiandrosterone (see Scheme 1, for recently reported examples).^[4] The steroidal analogues obtained show diverse pharmacological applications due to their effects on sex hormones, immune response, cell proliferation and because of their neuroactive properties. Given the bifunctional nature of the testosterone substrate, both the esterification of the hydroxyl group at C17 and the selective reduction of the carbonyl group present at C3 are two important transformations leading to pharmacologically active testosterone derivatives.^[5] Common to these reactions is the use of Lewis acid sites for the activation of carbonyl groups in the reactants, improving the yields of the desired products.^[6-8] However, homogeneously catalyzed transformations of testosterone also produce dehydration by-products, form soaps which consume the organic acid reactant and the reuse of the catalyst is not possible.^[9a-d] In this sense, heterogeneous catalysts have been reported for a few steroid transformations, with the esterification as the most widely described reaction.^[10] These heterogeneous catalysts are typically active, stable and easily recovered but their lower selectivity, high temperatures of operation and the formation of side-products are important drawbacks.



Scheme 1. Transformations of testosterone (1st and 2nd) and epiandrosterone (3rd and 4th) steroids involving the activation of carbonyl groups, together with the particular stoichiometric^{[9a],[9k]} or catalytic conditions^{[8b],[9g]} employed.

[a] Dr. F. G. Cirujano, C. Van Goethem, Prof. I.F.J. Vankelecom, Prof. D. E. De Vos

Centre for Surface Chemistry and Catalysis
KU Leuven Celestijnenlaan 200F, 3001 Leuven (Belgium)
E-mail: francisco.garcia@kuleuven.be; dirk.devos@kuleuven.be

[b] Dr. I. Luz, Dr. M. Soukri, Dr. M. Lail
RTI International
Research Triangle Park, NC 27709-2194 (USA)
E-mail: msoukri@rti.org

[*] These authors contributed equally to this work.

Supporting information for this article is given via a link at the end of the document

The design of highly active, reusable and selective heterogeneous catalysts is crucial to perform these transformations under mild and clean conditions, inspired by the catalytic efficiency of natural enzymes.^[11] Here we focus our attention on hexanuclear Zr(IV) oxoclusters as catalytically active sites due to their relatively low price and minimum toxicity, especially when immobilized in a solid support.^[12] Thus, (Zr)UiO-66(NH₂) was selected to be grown within the ordered monodimensional channels of SBA-15 based on the already reported reaction rate enhancement when using this MOF as acid-base catalyst.^{[2b],[13]} This is due to the fact that its linker content is generally lower than that expected for the ideal stoichiometric MOF (missing linker defects), generating hydrophilic Zr defect sites with acid character in addition to the Zr⁴⁺-O²⁻ acid-base pairs present in the (Zr)UiO-66(NH₂).^[7a-f]

The broad XRD peak around $2\theta \sim 7-8^\circ$ of the resulting (Zr)UiO-66(NH₂)/SBA-15 seems to indicate the presence of UiO type MOF nanocrystals in the SBA-15 matrix, although it is difficult to discern the two characteristic peaks of UiO-66 due to the small size of the crystals (see Figure S1). When the MOF synthesis was performed under the same conditions but in the absence of the SBA-15 matrix, slightly larger (15-20 nm, according to the Scherrer equation) UiO-66-NH₂ nanocrystals were obtained. This supports that the MOF is formed under the mild conditions proposed here for the (Zr)UiO-66(NH₂)/SBA-15 hybrid catalysts (see Figure S2a). TEM images show the selective loading of the SBA-15 monodimensional channels (9 nm) with (Zr)UiO-66(NH₂) (~5 nm), although a smaller fraction of MOF crystals (~5-20 nm) were also observed outside the channels when increasing the MOF loading (see Figures 1a and S3). In fact, the lower contrast between the brighter channels and darker walls of SBA-15 and the presence of Zr, N and C obtained by EDX evidences the MOF formation in the channels of the SBA-15. Elemental analysis of the (Zr)UiO-66(NH₂)/SBA-15 samples are in agreement with the Zr:N ratio found in defective (Zr)UiO-66(NH₂) samples (see Table S2).^[2b]

Other characterization techniques were used to provide additional evidences of the formation of the MOF within the mesoporous scaffold. First, the UV-Vis spectra of the (Zr)UiO-66(NH₂)/SBA-15 show the two main peaks around 265 and 365 nm, attributed to the absorption of Zr-O clusters and ligand-based absorption in this MOF (Figure S4).^[13c-d] Second, the MOF decomposition temperature is similar for both the MOF and the hybrid material (see TGA in Figure S9). In addition, the FTIR spectra of the (Zr)UiO-66(NH₂)/SBA-15 completely match with several of the characteristic bands of the (Zr)UiO-66(NH₂), such as the medium N-H bending vibration at 1626 cm⁻¹ and the strong C-N stretching absorption indicative for aromatic amines at 1356 cm⁻¹ (Figure 1b).^{13b} Furthermore, N₂ physisorption also indicates the pore filling of the mesoporous SBA-15 channels since increasing MOF loading leads to a proportional drop in mesoporosity and pore size but not in microporosity (Figures 1c S6). Finally, STEM-HAADF confirms the homogeneous distribution of the MOF within the SBA-15 (Figure 1d). The EDX analysis qualitatively shows the uniform dispersion of Zr in the siliceous matrix and moreover quantitatively determines a Zr:Si ratio of 0.19, which fairly coincides with the Zr:Si ratio of 0.16 determined by XRF.

The (Zr)UiO-66(NH₂)/SBA-15 solids at varying MOF loadings

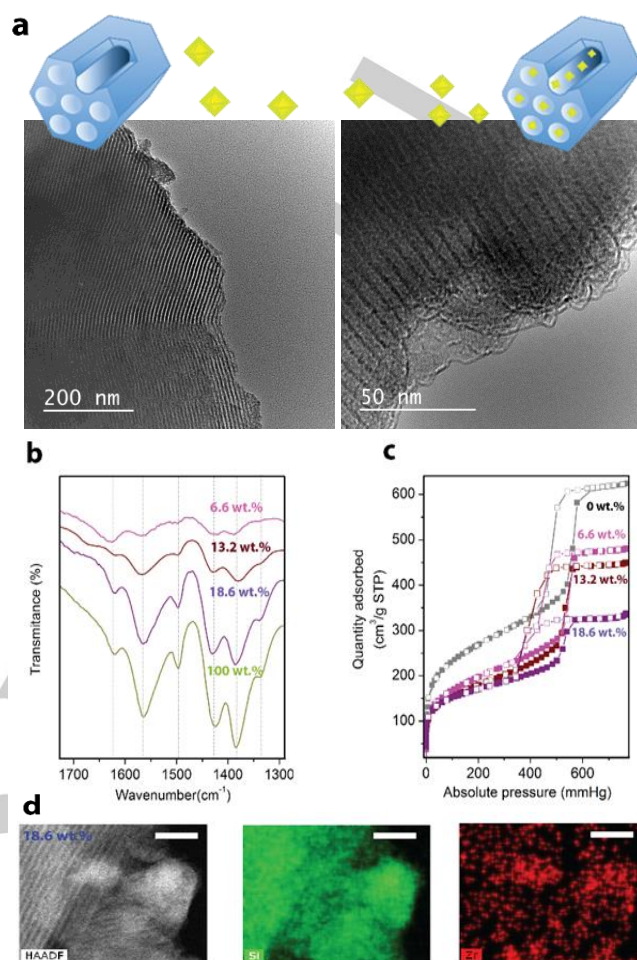


Figure 1. TEM images (a), FTIR spectra (b), N₂ physisorption (c) and EDX mapping (scale bar = 50 nm) (d), indicating the filling of the SBA-15 channels with (Zr)UiO-66(NH₂).

were tested as catalysts in the testosterone esterification to produce the testosterone caprylate **1** derivative. For comparison, the catalyst weight of all the materials was adjusted to use the same Zr concentration for all the reactions. The highest catalytic activity in the esterification of testosterone is obtained with the hybrid material containing the lowest amount of MOF (6.6 wt.%), with complete conversion to the desired ester **1** after 48 h (Figures 2 and S12). The advantage of using the mesoporous silica component is confirmed by the higher TOF obtained with the hybrid material (0.38 h⁻¹) with respect to those obtained with the similar MOF sample in the absence of SBA-15, following the method proposed here (0.19 h⁻¹) or by solvothermal reaction in DMF (0.16 h⁻¹). In fact, the reaction rate was increased up to 140% by using the catalyst containing 6.6 wt.% of MOF compared to the one containing 18.6 wt.%, and the rate was almost 230% higher than with the bulk MOF (see TOF values in Figure 2, right part).^[14] These results demonstrate that Zr catalytic sites in the well-dispersed MOF nanocrystals confined within the mesoporous matrix are more active than those present in the microporous bulk MOF because the latter are less available to interact with bulky reactants such as testosterone.

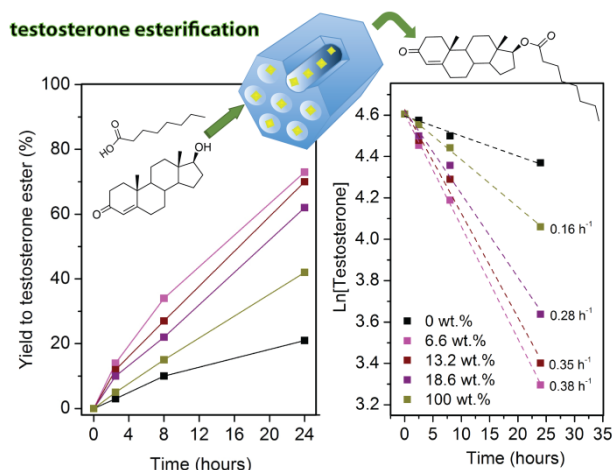


Figure 2. Testosterone esterification with caprylic acid catalyzed by (Zr)UiO-66(NH₂)/SBA containing varying MOF loadings (6.6, 13.2 and 18.6 wt.%) compared to bare SBA-15 and bulk MOF (100 wt.%). Yields of testosterone caprylate obtained by esterification of testosterone (left) and TOF values calculated for all the catalysts employed (right). Reaction conditions: 75 °C, 5 wt.% Zr with respect to testosterone, testosterone:caprylic acid molar ratio 1:20

It is noteworthy that the catalytic activity of the 6.6 wt.% (Zr)UiO-66(NH₂)/SBA-15 is practically the same after a second reaction cycle (92% yield), although some gradual decay is observed in subsequent runs (77% yield after seven reaction cycles). Less than 1% leaching of Zr from the solid catalyst was detected by ICP analysis of the liquid reaction medium after 24 h. Moreover, a hot filtration test of the solid catalyst slows down the reaction to a similar rate as the blank (autocatalytic) reaction, showing conversions similar to those measured for the blank reaction, thus demonstrating that the catalytic process is heterogeneous (Figure S13).

The benefits of using the (Zr)UiO-66(NH₂)/SBA-15 hybrid composite as catalyst with respect to bulk microporous inorganic or metal-organic solids are clear when large substrates such as testosterone are involved. To prove this, the esterification of a smaller substrate, such as 4-methylcyclohexanol, with octanoic acid was carried out by using the same reaction conditions and in the presence of 6.6 wt.% (Zr)UiO-66(NH₂)/SBA-15, bulk MOF and Zr-Beta zeolite, which exhibit similar pore dimensions as the MOF (6–7 Å). The ratio between the rate constant for esterification of testosterone and 4-methylcyclohexanol ($\varnothing = K_{\text{testosterone}}/K_{\text{cyclohexanol}}$) reveals a drop in the esterification rate for bulky substrates when the reaction is catalyzed by microporous catalysts, that is, bulk MOF ($\varnothing = 0.6$) and Zr-Beta ($\varnothing = 0.2$), compared to the hybrid material ($\varnothing = 1.2$), which exhibits the same or even a slightly higher catalytic activity for the bulky substrate, as shown in Figure S15 and Table S4. These ratios quantitatively demonstrate that the esterification of testosterone is catalyzed by those sites located at the outer surface of the crystal, which activity is notably boosted when the MOF is grown within SBA-15. Adsorption of testosterone was performed on all of the porous catalysts included in this work (see supporting information), resulting in 67 wt.%, 57 wt.%, 32 wt.% and 8 wt.% of testosterone uptakes for the same mass of SBA-15, 18.6

wt.% MOF/SBA-15, bulk MOF and Zr-Beta, respectively. The increased testosterone concentration at the active sites of the MOF/SBA-15 hybrid solid makes those sites more available to interact with the bulky testosterone reactant,^[19] enhancing its catalytic activity with respect to the bulk MOF in the absence of the mesoporous silica component.

To compare with a traditional ZrO₂-SBA-15 material, ZrO₂ nanocrystals confined within SBA-15 were obtained by calcining the 6.6 wt.% (Zr)UiO-66(NH₂)/SBA-15 to maintain the same concentration and dispersion. Remarkably, hexanuclear Zr oxoclusters located at the nodes of MOF nanocrystals exhibit a much better performance than the metal oxide nanocrystals resulting from calcination (TOFs of 0.38 h⁻¹ vs 0.15 h⁻¹, respectively), demonstrating the advantage of using MOF hybrid materials as heterogeneous catalysts instead of traditional supported metal oxide nanoparticles for this specific reaction of high pharmaceutical interest (Figure S12). Moreover, when the aim is the large-scale development of MOF/SiO₂ hybrid catalysts, the use of commercially available non-regular mesoporous silica (Silica(A)) exhibit excellent characteristics to meet some of the basic requirements for large scale industrial application, meeting the DOE's target price of 10 \$/Kg MOF.^{[3],[15]} In this way, comparable catalytic activity was measured for 10.2 wt.% MOF nanocrystals on Silica(A) with respect to that of 13.2 wt.% MOF on SBA-15 (0.33 h⁻¹ vs 0.35 h⁻¹, see table S3). Therefore, although this study mainly focuses on SBA-15 matrix, these results encourage further research in the use of alternative silica (or other matrices) to grow catalytically active MOF nanoparticles. In fact, the 10.2 wt.% (Zr)UiO-66(NH₂)/Silica(A) has been used as a stable and active catalytic packing for the esterification of octanoic acid with *n*-heptanol operating in continuous mode (Figure S26).

At this point, we also wanted to extend the scope of steroid transformations to further confirm the enhanced catalytic performance for the (Zr)UiO-66(NH₂)/SiO₂ hybrid catalysts with respect to the bulk MOF. A resume of this scope is shown in Figure 3 and Scheme S1. As demonstrated for testosterone esterification, superior catalytic performance and good stability were found for MOF hybrids in all cases (see details in Figures S16–S25). Hence, we also carried out the selective reduction of testosterone into androst-4-ene-3,17-diol **2**. The most widely

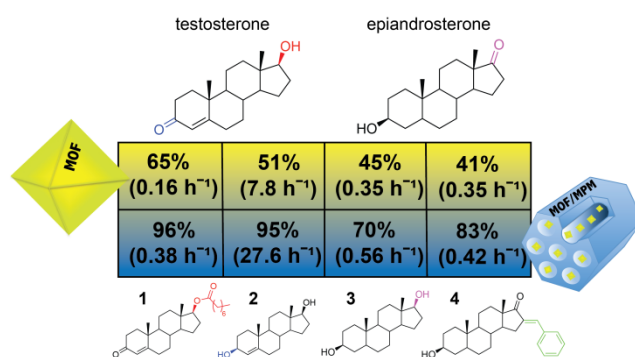


Figure 3. Resume of the catalytic performance, yield and (TOF) for the bulk MOF compared to 6.6 wt.% (Zr)UiO-66(NH₂)/SBA-15 in the synthesis of **1**, **2**, **3** and **4**. The reactions were carried out at 75 °C during 48 h for **1** and **24** h for **3** and **4**, while the synthesis of **2** was performed at room temperature for 0.75 h.

applied procedure is based on the use of NaBH₄ as reducing agent in the presence of stoichiometric amounts of Lewis acid, as in the Luche reduction conditions, to obtain a high selectivity for the allylic alcohol rather than for the saturated ketone or alcohol.^[9c-d,16] Herein we substitute the use of homogeneous catalysts by our heterogeneous hybrid catalysts, employing for the first time Zr as a Lewis acid in catalytic amounts (only 5 wt.% of Zr with respect to testosterone) for this particular reaction. Use of 6.6 wt.% (Zr)UiO-66(NH₂)/SBA-15 catalysts leads to the desired androst-4-ene-3,17-diol in quantitative yield and excellent chemoselectivity (95%) after just one hour of reaction at room temperature (see Figure S16 and Table S6).

Beside esterification and NaBH₄ reduction of testosterone, we explored the hydrogen transfer and aldol condensation reactions using epiandrosterone (5 α -androstan-3 β -ol-17-one) as a substrate. Different promoters or catalysts have been used to successfully carry out these two transformations (3rd and 4th transformations in Scheme S1).^[8,9g-i] On the one hand, using the 6.6 wt.% MOF loaded SBA-15, the catalytic hydrogen transfer from isopropanol to the carbonyl group of epiandrosterone produces the androstanediol **3** in 70% yield after 24 h (Figure S21) while only 45% was measured for bulk MOF. On the other hand, we tested the activity of the hybrid MOF/MPM in the synthesis of 16-(E)-benzylidene-androsterone **4** by aldol condensation with benzaldehyde, which is an intermediate in the synthesis of (spiro) heterocyclic steroids (see Scheme S3). In fact, the alteration of the chemical and biological properties of epiandrosterone by insertion of carbon atoms makes compound **4** a versatile intermediate or even a final product in the synthesis of novel anticancer drugs.^[9h-i] Thus, using the 6.6 wt.% loaded catalyst, the aldol condensation between epiandrosterone and benzaldehyde produces 83% yield of **4** with respect to the 41% obtained in the presence of the bulk MOF after 24 h (Figure S23). The hybrid material also preserves the major part of its activity in further reuses, obtaining 73% yield of **4** after five reaction runs (Figure S24).

In conclusion, we have demonstrated the superior catalytic performance of the MOF/MPM materials with respect to bulk microporous solids for the transformation of steroids, generating pharmaceutically interesting compounds. The use of such novel heterogeneous catalysts containing catalytically active MOF nanocrystals on mesoporous supports, will encourage the adoption of this approach for other applications. The increased catalytic activity and mechanical stability of this hybrid MOF nanocatalysts confined in the mesoporous scaffolds allows for multiple reuse of the catalyst without significant leaching of the active sites in batch and in continuous mode, important for its commercial use in industrial processes.

Experimental Section

Procedure for solid state crystallization of (Zr)UiO-66(NH₂) within SBA-15

First, a ligand salt precursor solution (TEA)₂BDC(NH₂) was used to impregnate the evacuated SBA-15. After drying at 50 °C under vacuum for 2 h, the resulting [(TEA)₂BDC(NH₂)/SBA-15] was treated with a nitrogen flow saturated with concentrated HCl (37%) for 2 hours at room

temperature. Afterwards, a metal salt precursor solution of ZrOCl₂·8H₂O in water was used to impregnate the [H₂BDC(NH₂)/SBA-15] mesoporous silica. The [ZrOCl₂/H₂BDC(NH₂)/SBA-15] solid was finally dried at 50 °C under vacuum in a rotavapor for 2 h and heated in an oven at 120 °C for 2 h. Finally it was washed with water and MeOH and dried overnight at 120 °C under vacuum (see supporting information for details).

Catalytic tests for steroid transformations

The specific amount of catalyst was added to a vial containing the reactants and *n*-tetradecane as the internal standard (see supporting information for details of each specific reaction). The suspension was stirred at the required temperature and sample aliquots were taken from the supernatant at different reaction times. The supernatant solution was analyzed with GC-FID.

Acknowledgements

Marie-Curie Individual Fellowship (MSCA-IF 750391-SINMOF) program, Flemish government (Methusalem CASAS2), FWO, Belspo (IAP-PAI 7/05) and Flemish Agency for Innovation through Science and Technology (IWT) are acknowledged for financial support. Funding for the TEM through Hercules project AKUL/13/19 is kindly acknowledged.

Keywords: mesoporous silica • nanoMOF • steroid chemistry • active site confinement • MOF composite

- [1] (a) A. Corma, H. García, F. X. Llabrés i Xamena, *Chem. Rev.* **2010**, *110*, 4606-4655; (b) P. Valvekens, F. Vermoortele, D. E. De Vos, *Catal. Sci. Technol.* **2013**, *3*, 1435-1445; (c) A. Dhakshinamoorthy, M. Opanasenko, J. Cejka, Jiri, H. Garcia, *Catal. Sci. Technol.* **2013**, *3*, 2509-2540; (d) J. Jiang, O. M. Yaghi, *Chem. Rev.* **2015**, *115*, 6966-6997; (e) B. Seoane, S. Castellanos, A. Dikhtiarenko, F. Kapteijn, J. Gascon, *Coord. Chem. Rev.*, **2016**, *307*, 147-187; (f) L. Chen, R. Luque, Y. Li, *Chem. Soc. Rev.* **2017**, *46*, 4614-4630; (g) S. Roy, C. B. George, M. A. Ratner, *J. Phys. Chem. C* **2012**, *116*, 23494-23502.
- [2] (a) F. Vermoortele, B. Bueken, G. Le Bars, B. Van de Voorde, M. Vandichel, K. Houthoofd, A. Vimont, M. Daturi, M. Waroquier, V. Van Speybroeck, C. Kirschhock, D. E. De Vos, *J. Am. Chem. Soc.* **2013**, *135*, 11465-11468. (b) F. G. Cirujano, A. Corma, F. X. Llabrés i Xamena, *Chem. Eng. Sci.* **2015**, *124*, 52-60; (c) O. Kozachuk, I. Luz, F. X. Llabrés i Xamena, H. Noei, M. Kauer, H. B. Albada, E. D. Bloch, B. Marler, Y. Wang, M. Muhler, R. A. Fischer, *Angew. Chem. Int. Ed.* **2014**, *53*, 7058-7062; (d) J. Canivet, M. Vandichela, D. Farrusseng, *Dalton Trans.* **2016**, *45*, 4090-4099; (e) A. K. Cheetham, T. D. Bennett, F. X. Coudert, A. L. Goodwin, *Dalton Trans.* **2016**, *45*, 4113-4126.
- [3] I. Luz, M. Soukri, M. Lail, *Chem. Mater.* **2017**, DOI: 10.1021/acs.chemmater.7b02042.
- [4] (a) A. Kucharchuk, P. Merrill, *WO03049732*; (b) O. Dhingra, J. S. Bernstein, *US20130303495*; (c) E. Dadey, L. G. Myers, M. A. Schobel, *WO2014144366*; (d) R. E. Dudley, P. P. Constantinides, *WO2006113505*; (e) S. Simes, M. Snabes, J. Zborowski, *US20120022033*; (f) B. Ranju, S. Guleria, G. Narang, R. W. Hartmann, *US2009137541*; (g) C. N. Ahlem, J. M. Frincke, L. D. Dos Anjos De Carvalho, W. Heggie, P. T. Prendergast, C. L. Reading, K. P. Thadikonda, R. N. Vernon, *US20030060425*; (h) J. P. Kutney, H. Chen, D. Hou, C. Wang, Changqing, *US20030232797*; (i) E. Wuelfert, J. R. Murray, D. Wynick, *MX2008006440*; (j) D. Covey, *US20150361125*.
- [5] (a) D. Qianchun, Z. Pin, H. Qingde, H. Fenghong, W. Fang, Z. Mingming, Y. Xiao, Z. Qi and Z. Chang, *Eur. J. Lipid Sci. Technol.* **2011**, *113*, 441-449. (b) W.-S. He, Y. Ma, X.-X. Pan, J.-J. Li, M.-G. Wang, Y.-B. Yang, C.-S. Jia, X.-M. Zhang B. Feng, *J. Agric. Food Chem.* **2012**, *60*, 9763-9769. (c) E. Jari, *US2002045773*; (d) L. Liu, *US20026413571*; (e) R. Allan, W. L. James, R. Bruce, F. Detraino, M. H. Boyer, J. D III Higgins, *PT982316*; (f) X. Meng, Q. Pan, T. Yang, *J. Am. Oil Chem Soc.* **2011**, *88*, 143-149; (g) S. Dugar, G. F. Schreiner, D. Mahajan, A. Sharma, R. I. Patil, B. Kuila, *WO2014115167*; (h) S. C. Manolagas, J. A. Bogen, *WO03002058*.

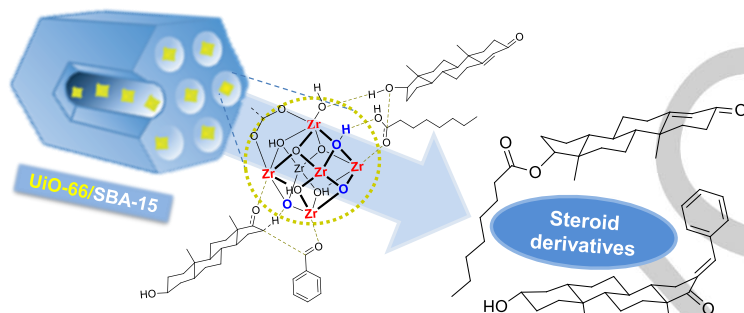
- [6] (a) A. Corma, M. E. Domine, L. Nemeth, S. Valencia, *J. Am. Chem. Soc.* **2002**, *124*, 3194-3195; (b) A. Corma, M. E. Domine, S. Valencia, *J. Catal.* **2003**, *215*, 294-304; (c) A. Corma, H. García, *Chem. Rev.* **2002**, *102*, 3837-3892; (d) A. Corma, H. García, *Chem. Rev.* **2003**, *103*, 4307-4366; (e) A. Corma, H. García, *Adv. Synth. Catal.* **2006**, *348*, 1391-1412.
- [7] (a) F. Vermoortele, R. Ameloot, A. Vimont, C. Serre, D. De Vos, *Chem Commun.* **2011**, *47*, 1521-1523; (b) V. N. Panchenko, M. M. Matrosova, J. Jeon, J. W. Jun, M. N. Timofeeva, S. H. Jung, *J. Catal.* **2014**, *316*, 251-259; (c) J. Hajek, M. Vandichel, B. Van de Voorde, B. Bueken, D. De Vos, M. Waroquier, V. Van Speybroeck, *J. Catal.* **2015**, *331*, 1-12; (d) J. F. Blandez, A. Santiago-Portillo, S. Navalon, M. Gimenez-Marques, M. Alvaro, P. Horcajada, H. Garcia, *J. Mol. Catal. A* **2016**, *425*, 332-339; (e) J. Hajek, B. Bueken, M. Waroquier, D. De Vos, V. Van Speybroeck, *ChemCatChem* **2017**, *9*, 2203-2210; (f) C. Caratelli, J. Hajek, F. G. Cirujano, M. Waroquier, F. X. Llabrés i Xamena, V. Van Speybroeck, *J. Catal.* **2017**, *352*, 401-414; (g) F. G. Cirujano, A. Corma, F. X. Llabrés i Xamena, *Catalysis Today* **2015**, *257*, 213-220; (h) I. Luz, C. Rösler, K. Epp, F. X. Llabrés i Xamena, R. A. Fischer, *Eur. J. Inorg. Chem.* **2015**, *23*, 3904-3912; (i) M.G. Goesten, J. Juan-Alcaniz, E.V. Ramos-Fernandez, K.B. Sai Sankar Gupta, E. Stavitski, H. van Bekkum, J. Gascon, F. Kapteijn, *J. Catal.* **2011**, *281*, 177-187.
- [8] (a) E. Plessers, G. Fu, C. Yong Xiang Tan, D. De Vos, M. B. J. Roefsaers, *Catalysts* **2016**, *340*, 136-149; (b) M. De bruyn, S. Coman, R. Bota, Vasile I. Parvulescu, D. De Vos, P. A. Jacobs, *Angew. Chem. Int. Ed.* **2003**, *42*, 5333-5336; (c) M. De bruyn, D. E. De Vos, P. A. Jacobs, *Adv. Synth. Catal.* **2002**, *344*, 1120-1125, (d) J. Iglesias, J. A. Melero, G. Morales, J. Moreno, Y. Segura, M. Paniagua, A. Cambra, B. Hernández *Catalysts* **2015**, *5*, 1911-1927; (e) M. D. Gracia, A. M. Balu, J. M. Campelo, R. Luque, J. M. Marinas, A. A. Romero, *Appl. Catal. A* **2009**, *371*, 85-91.
- [9] (a) F. Aiello, A. Garofalo, A. M. Aloisi, S. Lamponi, A. Magnani, A. Petroni, *J. Endocrinol. Invest.* **2013**, *36*, 390-395; (b) P. Marwah, A. Marwah, H. A. Lardy, *Tetrahedron* **2003**, *59*, 2273-2287; (c) J. L. Luche, L. Rodriguez-Hahn, P. Crabbé, *Chem. Commun.* **1978**, *14*, 601-602; (d) N. V. Forkel, D. A. Henderson, M. J. Fuchter, *Green Chem.* **2012**, *14*, 2129-2132; (e) P. Magnus, M. R. Fielding, *Tetrahedron Lett.* **2001**, *42*, 6633-6636; (f) N. Kennedy, T. Cohen, *J. Org. Chem.* **2015**, *80*, 8134-8141; (g) F. Alonso, P. Riente, M. Yus, *Tetrahedron* **2008**, *64*, 1847-1852; (h) H. Guoa, H. Wu, J. Yang, Y. Xiao, H.-J. Altenbach, G. Qiu, H. Hu, Z. Wu, X. He, D. Zhou, X. Hu, *Steroids* **2011**, *76*, 709-723; (i) A. Arenas-González, L. A. Mendez-Delgado, P. Merino-Montiel, J. M. Padrón, S. Montiel-Smith, J. L. Vega-Báez, S. Meza-Reyes, *Steroids* **2016**, *116*, 13-19; (j) A. Romero-López, S. Montiel-Smith, S. Meza-Reyes, P. Merino-Montiel, J. L. Vega-Baez, *Steroids* **2014**, *87*, 86-92; (k) S. Kanchithalaivan, R. R. Kumar, S. Perumal, *Steroids* **2013**, *78*, 409-417; (l) G. M. Allan, H. R. Lawrence, J. Cornet, C. Bubert, D. S. Fischer, N. Vicker, A. Smith, H. J. Tutill, A. Purohit, J. M. Day, M. F. Mahon, M. J. Reed, B. V. L. Potte, *J. Med. Chem.* **2006**, *49*, 1325-1345.
- [10] (a) S. Robles-Manuel, J. Barrault, S. Valange, *C. R. Chimie* **2011**, *14*, 656-662; (b) Y. Yang, W. He, C. Jia, Y. Ma, X. Zhang, B. Feng, *J. Molec. Catal. A* **2012**, *357*, 39-43.
- [11] (a) T. Seo, P. M. Oelkers, M. R. Giattina, T. S. Worgall, S. L. Sturley, R. J. Deckelbaum, *Biochemistry* **2001**, *40*, 4756-4762; (b) G. Gondos, L. G. McGirr, C. R. Jablonski, W. Snedden, J. C. Orr, *J. Org. Chem.* **1988**, *53*, 3057-3059; (c) M. Chen, J. E. Drury, D. W. Christianson, T. M. Penning *J. Biol. Chem.* **2012**, *287*, 16609-16622.
- [12] (a) K. Ohtsuka, Y. Hayashi, M. Suda, *Chem. Mater.* **1993**, *5*, 1823-1829; (b) M. Nakayama, A. Sato, K. Ishihara, H. Yamamoto, *Adv. Synth. Catal.* **2004**, *346*, 1275-1279; (c) F. Vermoortele, M. Vandichel, B. Van de Voorde, R. Ameloot, M. Waroquier, V. Van Speybroeck, D. Vos, *Angew. Chem. Int. Ed.* **2012**, *51*, 4887-4890.
- [13] (a) J. H. Cavka, S. Jakobsen, U. Olsbye, N. Guillou, C. Lamberti, S. Bordiga, K. P. Lillerud, *J. Am. Chem. Soc.* **2008**, *130*, 13850-13851; (b) M. Kandiah, M. Hellner Nilsen, S. Usseglio, S. Jakobsen, U. Olsbye, M. Tilset, C. Larabi, E. A. Quadrelli, F. Bonino, K. P. Lillerud, *Chem. Mater.* **2010**, *22*, 6632-6640; (c) C. Gomes-Silva, I. Luz, F. X. Llabrés i Xamena, A. Corma, H. García, *Chem. Eur. J.* **2010**, *16*, 11133-11138; (d) A. Santiago Portillo, H. G. Baldoví, M. T. García-Fernandez, S. Navalon, P. Atienzar, B. Ferrer, M. Alvaro, H. Garcia, Z. Li, *J. Phys. Chem. C* **2017**, *121*, 7015-7024.
- [14] Reaction rates are expressed by the kinetic constant assuming a pseudo-first order reaction due to the 20:1 excess of acid with respect to testosterone.
- [15] D. De Santis, J. A. Mason, B. D. James, C. Houchins, J.R. Long, M. Veenstra, *Energy Fuels* **2017**, *31*, 2024-2032.
- [16] (a) J. L. Luche, *J. Am. Chem. Soc.* **1978**, *100*, 2226-2227; (b) A. L. Gemal, J. L. Luche, *J. Am. Chem. Soc.* **1981**, *103*, 5454-5459; (c) E. Jones-Mensah, L. A. Nickerson, J. L. Deobald, H. J. Knox, A. B. Ertel, J. Magolan, *Tetrahedron* **2016**, *72*, 3748-3753.

Entry for the Table of Contents (Please choose one layout)

Layout 1: MOF/SBA-15 for the synthesis of bioactive steroid derivatives

COMMUNICATION

Confined Zr-MOF
nanocrystals
enhances the
catalytic activity
and stability of
bulk MOF for
different
transformations of
bulky steroids



Author(s),
Corresponding
Author(s)*

Page No. – Page
No.

Title